# Design of an Industrial Distributed Controller Near Spatial Domain Boundaries

Stevo Mijanovic, Greg E. Stewart, Guy A. Dumont, and Michael S. Davies

ABSTRACT

This paper proposes modifications to an industrial paper machine cross-directional (CD) controller, initially designed assuming process spatial invariance, near the sheet edges where the assumption of spatial invariance is clearly violated. The resulting design problem is equivalent to a block-decentralized static output feedback problem. The proposed approach sequentially synthesizes each block, resulting in an internally stable loop with nominal performance and robustness criteria satisfied.

## I. INTRODUCTION

The assumption of spatial-invariance is necessary for the application of the many new tools [1], [2], [5], [12] developed for the analysis and controller synthesis of spatially distributed control systems. With this assumption, controller synthesis can be significantly simplified. However, when the controllers are implemented on real systems with a spatial domain of finite width, the actual spatial boundary conditions (BC) are invoked [3]. Because of the idealized BC assumed in the design process, there is no guarantee of performance or even stability around the boundaries. A class of bounded, spatially distributed systems with its boundary conditions, for which stability and performance are guaranteed after implementing a controller designed assuming spatial invariance of the process is presented in [7].

An industrial example of a spatially distributed, large scale, multivariable process is the paper machine cross-directional (CD) control system. A paper machine produces a sheet of paper up to $11m$ wide. The objective of CD control is to reduce the variations of the paper sheet properties of interest (which include weight, moisture content, and thickness) in the cross-direction (the direction perpendicular to sheet travel) as efficiently as possible [3], [4], [11]. Most often, each one of these properties is controlled with a separate controller using 30–300 identically constructed and evenly distributed actuators in the cross-direction. The scanning sensor is mounted downstream from the actuator array and measures the sheet properties at up to 2000 locations across the sheet. The CD component of the measurement profile is subsequently spatially low-pass filtered and downsampled to the actuator resolution.

Industrial CD controllers, of interest in this paper, are essentially 2D (spatio-temporal) filters, causal in time and noncausal in the spatial domain [5], [9], [12]. In particular, we will consider the case in which these systems have been tuned using a two-dimensional loop shaping technique[1] [11], [12]. The spatial invariance approximation is central to this technique. The two-dimensional loop shaping technique has been successfully introduced to the industry, and to date has been implemented on more than 100 paper machines worldwide. However, as the process characteristics are different around the edges from those in the rest of the sheet, the initially computed spatially-invariant CD controllers are modified near the sheet edges before implementation on a paper machine [9].

The main contribution of this paper is a novel approach to the redesign of CD controllers to accommodate spatial domain boundaries, where the initial controller has been computed assuming idealized periodic boundary conditions. The objective is stated in terms of a static output feedback (SOF) design problem via appropriately defined linear fractional transformations (LFTs). The subsequent design approach is based on a novel low-bandwidth SOF controller synthesis algorithm. The algorithm is sequentially implemented on two constant matrix components in the existing industrial controller, modifying the CD control law near spatial domain boundaries by directly taking into account the relevant control engineering criteria: closed-loop stability, performance, and robustness. The objective of this work was to prepare for an industrial trial, that has subsequently been completed [8].

The main characteristics of the paper machine CD control systems and the objective of this work are given in Section II. The new approach to CD control near spatial domain boundaries is detailed in Section III. An example is presented in Section IV and conclusions in Section V.

## II. PROBLEM STATEMENT

### A. Paper Machine CD Control

The standard model of a paper machine CD control system, subject to process output disturbances, is given by:

$$y(z) = G(z) \cdot u(z) + d(z), \quad u(z) = K(z) \cdot y(z) \qquad (1)$$

S. Mijanovic, G.A. Dumont, and M.S. Davies are with the Department of Electrical and Computer Engineering, University of British Columbia, 2356 Main Mall, Vancouver, B.C., Canada, V6T 1Z4 stevom,guyd,miked@ece.ubc.ca

G.E. Stewart is with Honeywell Process Solutions, 500 brooksbank Avenue, North Vancouver, B.C., Canada, V7J 3S4 greg.stewart@honeywell.com

[1]This is done for convenience as we will implement the proposed design on a controller tuned in this way. The proposed design only requires the original controller to be stabilizing.

where $y(z), u(z) \in \mathcal{C}^n$ ($\mathcal{C}$ - set of complex numbers) are the $\mathcal{Z}$-transforms of the output (measurement) profile and the input (actuator) profile respectively, and $d(z) \in \mathcal{C}^n$ is the $\mathcal{Z}$-transform of the process output disturbance. The objective of the CD controller $K(z) \in \mathcal{C}^{n\times n}$ is rejection of disturbances $d(z)$. The number of actuators $30 \leq n \leq 300$ as stated above.

The process model's transfer matrix $G(z) \in \mathcal{C}^{n\times n}$ can be written as:

$$G(z) = [I - Az^{-1}]^{-1}Bz^{-d} \tag{2}$$

where the constant matrices $A$ and $B \in \mathcal{R}^{n\times n}$ have a Toeplitz symmetric structure[2]:

$$\begin{aligned} A &= \text{toeplitz}\{a_0, 0, 0, \ldots, 0\} \\ B &= \text{toeplitz}\{b_0, b_1, \ldots, b_{l_b}, 0, \ldots, 0\} \end{aligned} \tag{3}$$

The coefficients modelling the spatial response $[b_0, \cdots, b_{l_b}]$, the discrete-time pole $a_0$, and the process model deadtime $d$ are identified from input-output paper machine data, e.g. using commercial software described in [6]. This structure and the use of a band-diagonal Toeplitz matrix $B$ in (2) is standard in the modelling of CD processes [4]. The structure of the industrial CD controller of interest in this paper, $K(z)$ in (1), is given by:

$$K(z) = [I - Dz^{-1}]^{-1}D \cdot C \cdot c(z) \tag{4}$$

with real matrices $C$ and $D \in \mathcal{R}^{n\times n}$, and scalar transfer function $c(z)$. The scalar transfer function $c(z)$ is a stable deadtime compensator known as the Dahlin controller in the process industries [11].

The two-dimensional loop shaping controller tuning technique, presented in [12], is based on approximating the process model as spatially-invariant by imposing spatially periodic boundary conditions. This amounts to approximating the process Toeplitz symmetric matrices $A$ and $B$ in (2)–(3), with the corresponding circulant symmetric matrices $A_{cs}, B_{cs} \in \mathcal{R}^{n\times n}$:

$$\begin{aligned} A_{cs} &= \text{toeplitz}\{a_0, 0, 0, \ldots, 0\} \\ B_{cs} &= \text{toeplitz}\{b_0, b_1, \ldots, b_{l_b}, 0, \ldots, 0, b_{l_b}, \ldots, b_1\} \end{aligned} \tag{5}$$

Such an approximation, physically speaking, is equivalent to assuming that the paper machine produces a tube rather than a sheet of paper. As a result of the assumed process spatial invariance, an optimal controller will also be spatially-invariant [12]:

$$\begin{aligned} C_{cs} &= \text{toeplitz}\{c_0, c_1, \ldots, c_{l_c}, 0, \ldots, 0, c_{l_c}, \ldots, c_1\} \\ D_{cs} &= \text{toeplitz}\{d_0, d_1, \ldots, d_{l_d}, 0, \ldots, 0, d_{l_d}, \ldots, d_1\} \end{aligned} \tag{6}$$

where the coefficients $[c_0, c_1, \ldots, c_{l_c}]$ and $[d_0, d_1, \ldots, d_{l_d}]$ are determined by the controller tuning, and specify the number of off-diagonal elements of the matrices $C$ and $D$ respectively.

[2]Denoted using MATLAB notation.

However, the physical reality is that the controller must be implemented on a process that is more accurately modelled by the Toeplitz matrices given in (3). As a result, the initially computed spatially-invariant controller $K(z)$, given with (4) and (6), is modified near the spatial domain boundaries before it is implemented in the industrial control system. The current industrial practice designs these modifications based on signal processing techniques for extending finite width signals: zero, average, and reflection padding [9]. Subsequently, the same control law is implemented near the boundaries as in the middle of the sheet. Unfortunately, such an *ad hoc* modification of the CD control law near the edges does not take into account closed-loop characteristics of the resulting control system, and can lead to seriously degraded performance (even instability) near spatial boundaries [9].

### *B. Objective of this work*

Let us define the modifications to the existing controller matrices in (4) in terms of additive matrix perturbations $\delta C, \delta D \in \mathcal{R}^{n\times n}$ in Fig. 1. The elements of $\delta C$ and $\delta D$ are given by,

$$[\delta C]_{ij} = \begin{cases} \delta c_{ij}, & 1 \leq i \leq n_{C1} \text{ and } n - n_{C1} + 1 \leq i \leq n \\ & 1 \leq j \leq n_{C2} \text{and } n - n_{C2} + 1 \leq j \leq n \\ 0, & \text{otherwise} \end{cases} \tag{7}$$

$$[\delta D]_{ij} = \begin{cases} \delta d_{ij}, & 1 \leq i \leq n_{D1} \text{ and } n - n_{D1} + 1 \leq i \leq n \\ & 1 \leq j \leq n_{D2} \text{and } n - n_{D2} + 1 \leq j \leq n \\ 0, & \text{otherwise} \end{cases} \tag{8}$$

with $l_c \leq n_{C1} \leq n/2$, $l_d \leq n_{D1} \leq n/2$, and $1 \leq n_{C2}, n_{D2} \leq n$. However, most often $n_{C1}, n_{C2}, n_{D1}, n_{D2} \ll n$, resulting in only the upper-left and lower-right corners of the matrices $\delta C$ and $\delta D$ being different from zero. The parameters $l_c$ and $l_d$ are the respective widths of the matrix bands of $C$ and $D$ in (6).

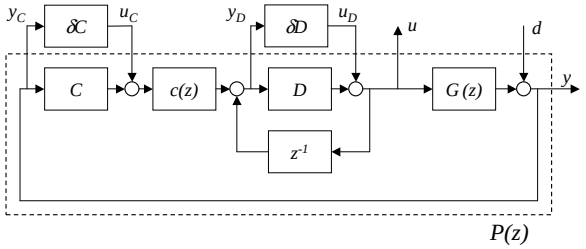


Fig. 1. CD control system with control law modifications, $\delta C$ and $\delta D$, near the sheet edges.

By factoring out controller perturbations $\delta C$ and $\delta D$ as shown in Fig. 1, a lower linear fractional transformation (LFT) as illustrated in Fig. 2, can be defined. The generalized plant $P(z)$ in Fig. 2 consists of the closed-loop transfer functions that can be obtained, after some straightforward algebra, from the system shown in Fig. 1.

As pointed out in Section II-A, the modifications $\delta C$ and $\delta D$ currently used in industrial CD control systems do not take into account relevant control engineering criteria

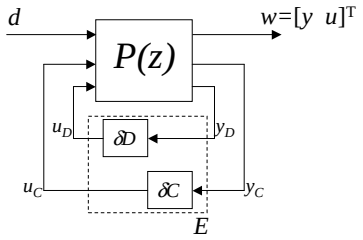


Fig. 2. Problem reformulated in terms of linear fractional transformation (LFT).

and can lead to very poor control near spatial domain boundaries.

The objective of this work is to find a block-diagonal compensator $E$ in Fig. 2, such that:
**(1)** $\delta D, \delta C \in \mathcal{R}^{n\times n}$ are static matrices with $n_{C1}, n_{C2}, n_{D1}, n_{D2} \ll n$ in (7) and (8).
**(2)** The resulting closed-loop system is stable.
**(3)** The closed-loop performance of the system, as measured by the 2-norm of the process output vector at low frequencies, is improved:

$$\|y(e^{j\omega}, E)\|_2 < \|y(e^{j\omega}, 0)\|_2, \quad \forall\, |\omega| < \omega_b, \tag{9}$$

for some $\omega_b > 0$.
**(4)** The gain $M(e^{j\omega}, E) : d \to u$ is limited across all the frequencies, i.e. for a given weight $W(e^{j\omega}) > 0$:

$$\overline{\sigma}(M(e^{j\omega}, E)) < W(e^{j\omega}), \quad \forall\, \omega, \tag{10}$$

where $\overline{\sigma}(\cdot)$ denotes the maximum singular value.

The first requirement above is the consequence of the main objective of this work: designing a localized modification of the existing control law near the sheet edges without changing the controller structure. The need for the second requirement is obvious. The third requirement is in accordance with the main objective of CD control: the reduction of process output variations as measured by its vector 2-norm. The fourth requirement is a result of the desired preservation of the system robustness characteristics[3].

## III. Sequential Design of SOF Compensators

In this work the design of $\delta D$ and $\delta C$ in Fig. 2 will be performed sequentially as it is very difficult to design a static output feedback (SOF) compensator $E$ with an additional block-diagonal structure constraint[4]. A novel low-bandwidth SOF controller design algorithm, outlined in Section III-A, is used for computing CD controller modifications in Section III-B.

[3]In the two-dimensional loop shaping procedure, the process model uncertainty is modelled as additive uncertainty, and subsequently $\|K[I - GK]^{-1}\|_\infty$ is a measure of system robustness.

[4]A wide variety of SOF problems are analyzed in [13] and references therein.

### A. SOF controller synthesis

In this work, we are concerned with a stable, finite-dimensional generalized plant $N(z)$:

$$N(z) = \begin{bmatrix} N_{11}(z) & N_{12}(z) \\ N_{21}(z) & N_{22}(z) \\ N_{31}(z) & N_{32}(z) \end{bmatrix}, \tag{11}$$

illustrated in Fig. 3. The signal $d(z)$ represents the exogenous input, $w_a(z)$ and $w_b(z)$ represent the exogenous outputs, $y(z)$ represents the feedback signal, and $u(z)$ represents the control signal. Let the generalized plants $N_a(z)$ and $N_b(z)$ be defined as[5],

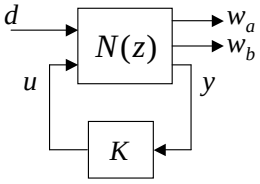


Fig. 3. Diagram of the lower linear fractional transformation $\mathcal{F}_l(N, K)$.

$$N_a = \begin{bmatrix} N_{11} & N_{12} \\ N_{31} & N_{32} \end{bmatrix}, N_b = \begin{bmatrix} N_{21} & N_{22} \\ N_{31} & N_{32} \end{bmatrix}, \tag{12}$$

then the input-output transfer functions, $d(z) \to w_a(z)$ and $d(z) \to w_b(z)$, are given by lower linear fractional transformations[5]:

$$\begin{aligned} \mathcal{F}_l(N_a, K) &= N_{11} + N_{12}K(I - N_{32}K)^{-1}N_{31} \\ \mathcal{F}_l(N_b, K) &= N_{21} + N_{22}K(I - N_{32}K)^{-1}N_{31} \end{aligned} \tag{13}$$

The objective is to design a compensator such that:
**(a)** the controller $K(z) = K_0$ is a static matrix,
**(b)** the feedback system with $K(z) = K_0$ is stable,
**(c)** the compensator improves the closed-loop performance as measured by the Frobenius norm,

$$\|\mathcal{F}_l(N_a(e^{j\omega}), K_0)\|_F < \|\mathcal{F}_l(N_a(e^{j\omega}), 0)\|_F, \tag{14}$$

$\forall\, |\omega| < \omega_b$, for some $\omega_b > 0$,
**(d)** the performance at higher frequencies is not overly degraded. In other words, a constraint,

$$\|\mathcal{F}_l(N_b(e^{j\omega}), K_0)\|_\infty < 1, \quad \forall\omega \tag{15}$$

is satisfied.
It can be seen that the above requirements (a)–(b) completely correspond to the requirements (1)–(2) in Section II-B. Also, the requirement (c) above is closely linked to the requirement (3), as the Frobenius norm is related to the sum of all singular values [10], and $\|y\|_2$ directly depends on the singular values of the corresponding closed-loop transfer function $d \to y$.

Since $N(z)$ in (11) is stable, the internal stability of the closed-loop system in Fig. 3 is equivalent to the input-output stability of $K(z)(I - N_{32}(z)K(z))^{-1}$ in (13). We can

[5]Transfer functions' argument $(z)$ is omitted for brevity.

then write down the familiar parametrization of stabilizing controllers $K(z)$ for the feedback system in Fig. 3,

$$K(z) = Q(z)(I + N_{32}(z)Q(z))^{-1} \quad (16)$$

for stable $Q(z)$ (see for example [14]), leading to the convenient form of the LFTs in (13),

$$\mathcal{F}_l(N_a(z), K(z)) = N_{11}(z) + N_{12}(z)Q(z)N_{31}(z) \quad (17)$$

$$\mathcal{F}_l(N_b(z), K(z)) = N_{21}(z) + N_{22}(z)Q(z)N_{31}(z) \quad (18)$$

Consider the low-frequency requirement on the Frobenius norm in (14). Using (17) we can write the LFT at steady-state ($\omega = 0$),

$$\mathcal{F}_l(N_a(e^{j0}), K(e^{j0})) = N_{11}(e^{j0}) + N_{12}(e^{j0}) \cdot Q(e^{j0}) \cdot N_{31}(e^{j0}) \quad (19)$$

Now consider the following optimization problem motivated by (19),

$$Q_0 = \arg\min_{Q \in \mathcal{R}} J(N_a(e^{j0}), \rho, Q)$$

$$J = \left\| N_{11}(e^{j0}) + N_{12}(e^{j0}) \cdot Q \cdot N_{31}(e^{j0}) \right\|_F^2 + \rho \left\| Q \right\|_F^2 \quad (20)$$

A closed-form solution to this optimization problem for a real static matrix $Q_0$ is given in [8]. Subsequently, the resulting $Q_0$ from (20) is used to form the static controller $K_0$ (requirement (a) above),

$$K_0 = Q_0(I + N_{32}(e^{j0})Q_0)^{-1} \quad (21)$$

The first term in optimization (20) is intended to address the above specified performance requirement (14), while the second term is intended to limit the magnitude of the synthesized matrix $Q_0$. The conditions on $\rho$ and generalized plant $N(z)$, such that the stability condition (b) and the dynamical condition (d) above are satisfied, are determined by Theorem 1 below. The closed-loop performance improvement (14), with the CD controller designed using the above outlined algorithm is guaranteed by Theorem 2.

*Theorem 1:* **(Stability and Full Bandwidth Performance Limit)** If $N(z)$ in (11) is stable, $\bar{\sigma}(\mathcal{F}_l(N_b(e^{j\omega}), 0)) < 1$ for all $\omega$, and $\rho > \beta$ in (20) where

$$\beta = \sqrt{r_{12} r_{31}} \cdot \bar{\sigma}(N_{12}(e^{j0}))\ \bar{\sigma}(N_{31}(e^{j0}))\ \bar{\sigma}(N_{11}(e^{j0})) \cdot \left\{ \left\| N_{32}(z) - N_{32}(e^{j0}) \right\|_\infty + \frac{\|N_{22}(z)\|_\infty \cdot \|N_{31}(z)\|_\infty}{1 - \|N_{21}(z)\|_\infty} \right\} \quad (22)$$

with the integers $r_{12}$ and $r_{31}$ denoting the rank of $N_{12}(e^{j0})$ and $N_{31}(e^{j0})$, respectively. Then $K_0$ synthesized from (20)–(21) stabilizes the feedback system in Fig. 3 and

$$\bar{\sigma}\big(\mathcal{F}_l(N_b(e^{j\omega}), K_0)\big) < 1, \qquad \text{for all } \omega \quad (23)$$

where $\bar{\sigma}(\cdot)$ denotes the maximum singular value.

*Proof*: Given in [8].

*Theorem 2:* **(Low Frequency Performance Improvement)** If $N(z)$ in (11) is stable, then for any $K_0 \neq 0$ constructed from (20)-(21) that stabilizes the system in Fig. 3, there exists a frequency $\omega_b > 0$ such that

$$\left\| \mathcal{F}_l(N_a(e^{j\omega}), K_0) \right\|_F < \left\| \mathcal{F}_l(N_a(e^{j\omega}), 0) \right\|_F \quad (24)$$

for all $|\omega| < \omega_b$.

*Proof*: Given in [8].

The value for the weight $\rho$ in (20) is determined through bisection on $\rho$ to produce a $K_0$ in (21) such that the requirements (b)–(d) are successfully traded off, and is initialized with the value computed based on Theorem 1. Subsequently, the bisection continues as long as the stability and full bandwidth requirements are satisfied, and until the difference between the two consecutive values of the weight $\rho$ in (20) is smaller than some specified value of the tolerance.

### B. Computing CD controller modifications

The first step in the proposed CD controller modification is a replacement of the initially computed spatially-invariant controller matrices $C_{cs}$ and $D_{cs}$ in (6) with their corresponding Toeplitz symmetric matrices. Next, the final controller modifications are computed using the SOF algorithm in turn on the $\delta D$ and $\delta C$ matrices in Fig. 1 and 2, presented in Section III-A. Since the SOF algorithm requires stable systems, the closed-loop stability of the system with Toeplitz symmetric process and controller models, is assumed. Based on numerous industrial data, as well as simulation studies, this is not a restrictive assumption and is only violated in certain pathological examples. However, if the system with Toeplitz symmetric process and controller models is not stable, then a stabilization procedure is required. Such a stabilization procedure is presented in [8].

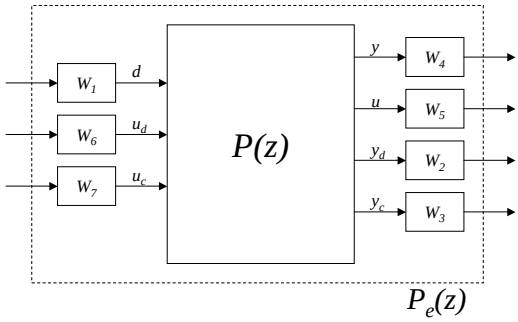


Fig. 4. Isolating system inputs/outputs near one edge.

Since the two edges of the paper machine are modelled to be identical, it is enough to retune the controller at one edge only. Subsequently, the corresponding modifications at the other edge can easily be found by symmetry arguments. Factoring out the control system inputs and outputs near one edge, based on the closed-loop system in Fig. 2, is performed with rectangular weights $W_i$, $i = 1, 2, \ldots, 7$, as illustrated in Fig. 4. The weighting matrices $W_i$ are defined

as:

$$W_2 = \underbrace{[\mathrm{I}_{n_{D1}}\ 0_{n_{D1}\times(n-n_{D1})}]}_{n_{D1}\times n},\quad W_3 = \underbrace{[\mathrm{I}_{n_{C1}}\ 0_{n_{C1}\times(n-n_{C1})}]}_{n_{C1}\times n},$$
$$W_4 = \underbrace{[\mathrm{I}_{n_y}\ 0_{n_y\times(n-n_y)}]}_{n_y\times n},\quad W_5 = \underbrace{[\mathrm{I}_{n_u}\ 0_{n_u\times(n-n_u)}]}_{n_u\times n},$$
$$W_1 = \underbrace{\begin{bmatrix} I_{n_d} \\ 0_{(n-n_d)\times n_d}\end{bmatrix}}_{n\times n_d},\quad W_6 = \underbrace{\begin{bmatrix} I_{n_{D2}} \\ 0_{(n-n_{D2})\times n_{D2}}\end{bmatrix}}_{n\times n_{D2}},$$
$$W_7 = \underbrace{\begin{bmatrix} I_{n_{C2}} \\ 0_{(n-n_{C2})\times n_{C2}}\end{bmatrix}}_{n\times n_{C2}} \qquad (25)$$

The matrices $W_2, W_3, W_6, W_7$ are used to convert the matrix sub-block design into a full-block design problem ($D_e = W_6^T \cdot \delta D \cdot W_2^T$, $C_e = W_7^T \cdot \delta D \cdot W_3^T$), i.e.,

$$[D_e]_{ij} = \delta d_{ij},\ \ 1 \le i \le n_{D1} \text{ and } 1 \le j \le n_{D2},$$
$$[C_e]_{ij} = \delta c_{ij},\ \ 1 \le i \le n_{C1} \text{ and } 1 \le j \le n_{C2}, \qquad (26)$$

where $\delta c_{ij}$ and $\delta d_{ij}$ are the same as those elements in (7)–(8). In other words, $C_e \in \mathcal{R}^{n_{C1}\times n_{C2}}$ and $D_e \in \mathcal{R}^{n_{D1}\times n_{D2}}$ are the non-zero, upper-left elements of the matrices $\delta C$ and $\delta D$ in (7)–(8), respectively. The matrices $W_1, W_4, W_5$, on the other hand, are used to isolate the sheet edges for consideration in the performance design.

The order of the transfer matrix $P_e(z)$ in Fig. 4 can easily reach into the thousands for practical systems. However, most of these states can be eliminated using the order reduction procedure based on Hankel singular values as they are mainly related to the inputs/outputs located in the middle of the sheet and the other machine edge. Based on the diagram given in Fig. 4, the linear fractional transformations (LFT's) for computing modifications $C_e$ and $D_e$ in (26) can be defined. They are presented in Fig. 5a and 5b. The design of $C_e$ and $D_e$ is performed by alternately synthesizing one matrix component while holding the other fixed. The synthesis procedure is the SOF method of Section III-A.

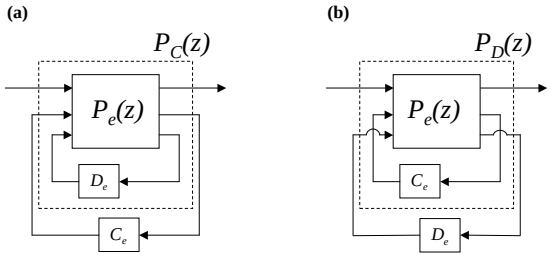


Fig. 5. Linear fractional transformations for sequentially computing (a) $C_e$ and (b) $D_e$ modifications.

## IV. Example

Simulation studies presented in this section were carried out using the real industrial identification and controller tuning software detailed in [6], [11] (residing on one computer), and a hardware-in-the-loop simulator (residing on another computer). The CD control system, presented below, describes an array of $n = 36$ slice lip actuators being used to control the paper sheet basis weight profile[6]. The parameters of the process model in (2)–(3) were identified using software described in [6] with the size of the matrix $B$ in (3) band $l_b = 6$ and

$$\{b_0, \ldots, b_6\} = 10^{-3} \cdot \{0.1652, 0.2044, 0.0789, -0.0382, -0.0169, -0.0009, 0.0001\}$$
$$a_0 = 0.855, \quad d = 2 \qquad (27)$$

The feedback controller $K(z)$ in (4) was designed using the standard two-dimensional loop shaping technique [11], [12]. The obtained controller parameters in (6) had matrix band sizes $l_c = 4, l_d = 1$, with:

$$\{c_0, \cdots, c_4\} = \{-0.2089, -0.2129, -0.0487, 0.0856, 0.0481\}$$
$$\{d_0, d_1\} = \{0.9878, 0.0061\} \qquad (28)$$

The parameters of the Dahlin controller $c(z)$ in (4) are also produced by the two-dimensional loop shaping design, but as not being central to this work, they are omitted here for brevity. Subsequently, the initially computed circulant-symmetric controller matrices are replaced with the corresponding Toeplitz symmetric matrices. After confirming stability of the system with the process and controller Toeplitz symmetric matrices, the procedure for modifying CD control near the edges, presented in Section III, can be implemented.

The closed-loop simulations have been performed with the steady-state process output disturbance, $d(z)$ in (1), as shown in Fig. 6. Near one edge (left side), the disturbance has a significant high spatial frequency content, and near the other (right side), has a smoother appearance. The first type of disturbance very often leads to system instabilities in real life CD systems as the actuator array attempts to remove the uncontrollable (high frequency) modes of the process output disturbance. The second type of disturbance (introduced near the right edge) is usually successfully attenuated by the control systems. The closed-loop simulation results

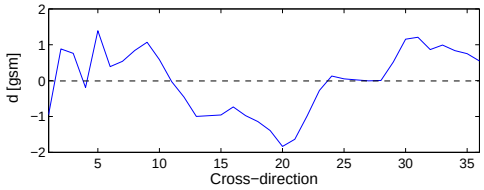


Fig. 6. Process output disturbance $d$ (at zero temporal frequency $\omega = 0$).

are shown in Fig. 7–10, and summarized in Table I. Fig. 7 illustrates the closed-loop steady-state process output and actuator profile using reflection padding (one of the techniques currently used in industry). Simulation results, with the controller tuned in turn conservatively, balanced,

[6]More details about the system can be found in [8].

and aggressively using the new approach from Section III, are given in Fig. 8 – 10. In all three cases, the sizes of the rectangular weights $W_i, i = 1, \ldots, 7$ in (25) were chosen as, $n_{C1} = 5, n_{C2} = 8, n_{D1} = 3, n_{D2} = 8, n_u = 8, n_d = 8, n_y = 8$, and the output vectors $w_a(z)$ and $w_b(z)$ in Fig. 3 as, $w_a(z) = [k_P y(z)\ u(z)]^T$, $w_b(z) = \frac{1}{1+k_R} u(z)$, where $y(z)$ and $u(z)$ are the process output and control signal respectively, and $k_P$ and $k_R$ are the tuning variables. For the CD process model given with (27), $\frac{1}{\overline{\sigma}(G(e^{j0}))} = 232.56$, where $\overline{\sigma}(\cdot)$ denotes the maximum singular value. The tuning variables, in the case of conservative tuning were chosen as: $k_P = 300$, $k_R = 0.2$, balanced tuning: $k_P = 1620$, $k_R = 0.2$, and in the case of aggressive tuning: $k_P = 2400$, $k_R = 0.5$.

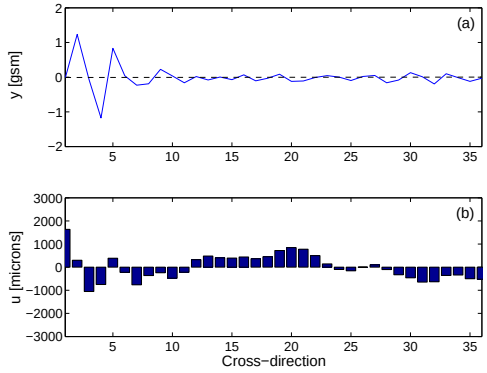


Fig. 7. Steady-state process output (a) and control signal (b), using the current industrial technique - reflection padding.

It can be seen from Fig. 8 – 10 and Table I that, by using the approach presented in Section III, a successful trade-off between performance (a flat CD profile) and the corresponding control signal magnitude, can be achieved. From Table I, it can be noticed that in case of all three tunings based on the new approach, the output profile has been improved in comparison to the result achieved with the existing technique. Also, in the cases of conservative and balanced tunings, such a result has been achieved with less actuator usage.

| | **Current method** | **New approach** (three different tunings) | | |
|---|---|---|---|---|
| | | Conservative | Balanced | Aggressive |
| $\|y\|_2$ | 1.9913 | 1.8305 | 1.4467 | 1.0577 |
| $\|u\|_2$ | 3307 | 2376 | 2974 | 4436 |

TABLE I

2-NORM OF THE PROCESS OUTPUT $y$ AND CONTROL SIGNAL $u$ STEADY-STATE PROFILES SHOWN IN FIG. 7 – 10.

## V. CONCLUSIONS

In this paper, a new approach to paper machine CD control near spatial domain boundaries has been presented. The new technique directly takes into account relevant control

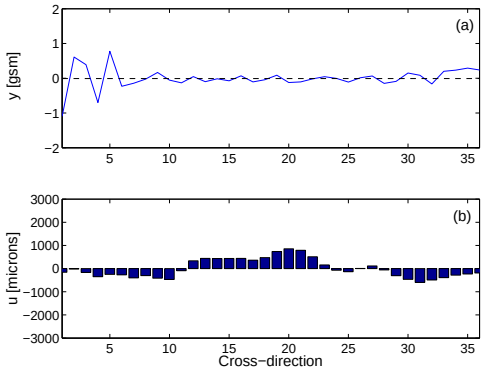


Fig. 8. Steady-state process output (a) and control signal (b), using the new technique - conservative tuning.

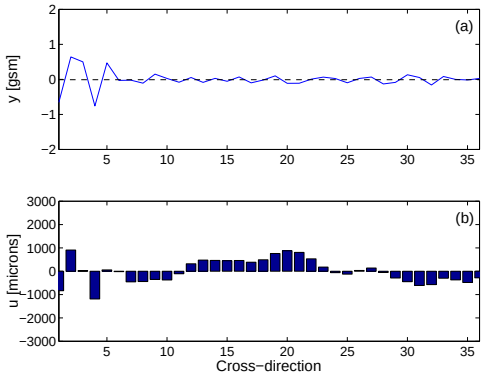


Fig. 9. Steady-state process output (a) and control signal (b), using the new technique - balanced tuning.

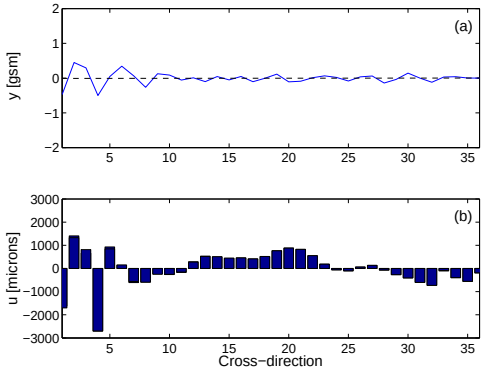


Fig. 10. Steady-state process output (a) and control signal (b), using the new technique - aggressive tuning.

engineering criteria: closed-loop stability, performance, and robustness.

Cross-directional controllers are often designed under the assumption of spatial invariance, which is clearly violated near spatial domain boundaries (paper machine edges). As a result, such controllers often result in an excessively large control signal originating from the spatial boundaries that can even lead to control system instability. The new

approach modifies the CD control law near the paper sheet edges by sequentially applying a low-bandwidth static output feedback design on two matrix components of the existing industrial controller, without changing the controller structure or complexity.

An example was presented of poor control near the edges, using the currently implemented technique in industry. It was illustrated that by implementing the newly developed technique, the results were substantially improved. With the new technique, it is possible to achieve the desired level of aggressiveness of CD controller near spatial domain boundaries. The new technique has also been successfully tested on a paper machine in a working paper mill [8].

## ACKNOWLEDGEMENTS

The financial support of the first author's work by the Natural Sciences and Engineering Research Council of Canada, the Science Council of British Columbia, and Honeywell Process Solutions - North Vancouver is gratefully acknowledged.

## REFERENCES

[1] B. Bamieh, F. Paganini, and M. Dahleh. Distributed control of spatially invariant systems. *IEEE Trans. on Automatic Control*, 47(7):1091–1107, July 2002.

[2] R. D'Andrea and G.E. Dullerud. Distributed control design for spatially interconnected systems. *IEEE Trans. on Automatic Control*, 48(9):1478–1495, September 2003.

[3] S.R. Duncan. *The cross-directional control of web forming processes*. PhD thesis, University of London, UK, 1989.

[4] A.P. Featherstone, J.G. VanAntwerp, and R.D. Braatz. *Identification and Control of Sheet and Film Processes*. Springer-Verlag, London, 2000.

[5] D.M. Gorinevsky, S. Boyd, and G. Stein. Optimization-based tuning of low-bandwidth control in spatially distributed systems. In *Proc. of American Control Conference*, pages 2658–2663, Denver, Colorado, USA, June 2003.

[6] D.M. Gorinevsky and C. Gheorghe. Identification tool for cross-directional processes. *IEEE Trans. on Control Systems Technology*, 11(5):629–640, September 2003.

[7] C. Langbort and R. D'Andrea. Imposing boundary conditions for a class of spatially-interconnected systems. In *Proc. of American Control Conference*, pages 107–112, Denver, Colorado, USA, June 2003.

[8] S. Mijanovic. *Paper Machine Cross-Directional Control Near Spatial Domain Boundaries*. PhD thesis, University of British Columbia, BC, Canada, 2004 (http://control.ece.ubc.ca/).

[9] S. Mijanovic, G.E. Stewart, G.A. Dumont, and M.S. Davies. Stability-preserving modification of paper machine cross-directional control near spatial domain boundaries. In *Proc. of IEEE Conference on Decision and Control*, pages 4113–4119, Las Vegas, Nevada, USA, December 2002.

[10] S. Skogestad and I. Postlethwaite. *Multivariable feedback control: analysis and design*. Wiley, New York, 1996.

[11] G.E. Stewart, D.M. Gorinevsky, and G.A. Dumont. Feedback controller design for a spatially-distributed system: The paper machine problem. *IEEE Trans. on Control Systems Technology*, 11(5):612–628, September 2003.

[12] G.E. Stewart, D.M. Gorinevsky, and G.A. Dumont. Two-dimensional loop shaping. *Automatica*, 39(5):779–792, May 2003.

[13] V.L. Syrmos, C.T. Abdallah, P. Dorato, and K. Grigoriadis. Static output feedback - a survey. *Automatica*, 33(2):125–137, February 1997.

[14] K. Zhou, J.C. Doyle, and K. Glover. *Robust and Optimal Control*. Prentice Hall, New Jersey, 1996.